

## LITERATURE CITED

- Hanna, O. T., and O. C. Sandall, "Developed Turbulent Transport in Ducts for Large Prandtl or Schmidt Numbers," *AIChE J.*, **18**, 527 (1972).
- Hughmark, G. A., "Wall Region Mass Transfer for Large Schmidt Numbers in Turbulent Pipe Flow," *ibid.*, **23**, 601 (1977).
- Notter, R. H., and C. A. Sleicher, "The Eddy Diffusivity in the Turbulent Boundary Layer Near a Wall," *Chem. Eng. Sci.*, **26**, 161 (1971).
- Sandall, O. C., O. T. Hanna, and M. Gelibter, "Turbulent Non-Newtonian Transport in a Circular Tube," *AIChE J.*, **22**, 1142 (1976).
- Shaw, D. A., and T. J. Hanratty, "Turbulent Mass Transfer Rates to a Wall for Large Schmidt Numbers," *ibid.*, **23**, 28 (1977).
- Shaw, D. A., "Mechanism of Turbulent Mass Transfer to a Pipe Wall at High Schmidt Number," Ph.D. thesis, Univ. Ill. (1976).

Manuscript received October 17, 1977; revision received April 20, and accepted June 8, 1978.

# Mathematical Models of the Monolith Catalytic Converter:

## Part III. Hysteresis in Carbon Monoxide Reactor

BRUCE A. FINLAYSON and LARRY C. YOUNG

Department of Chemical Engineering  
University of Washington  
Seattle, Washington 98195

Hysteresis is examined for monolith chemical reactors that are used to oxidize carbon monoxide in automobile exhaust. The term hysteresis refers to a multiplicity of steady states, and the actual steady state depends on the past history of operation of the reactor. In particular, different outlet conversions are obtained for the same inlet temperature depending on whether the device starts out hot or cold. A model developed earlier (Young and Finlayson, 1976a, b) used the collocation method to solve the equations for heat, mass, and momentum transfer in a single adiabatic channel of the monolith. Here we examine the influence of several operating and design parameters on the earlier results: velocity, inlet concentration, geometry of the duct, thermal conductivity of the wall, and effective diffusivity in the porous layer. We then compare the model to experimental data.

### MODEL

The basic model is the one described earlier (7, 8) as model II-A: a square duct with axial conduction longitudinally in the solid walls, but with infinitely fast conduction peripherally around the square, and including the diffusion of heat and mass in the transverse direction in the fluid. Nusselt and Sherwood numbers are not assigned a priori. The reaction rate expression is  $P_2$  in (8) with a basic form

$$\text{rate} = \frac{Dy_{O_2}y_{CO}e^{-A/T}}{(1 + C'y_{CO}e^{B/T})^2} = \frac{k_o(E + y)y}{(1 + \alpha y)^2} \quad (1)$$

This is the expression derived by Voltz et al. (1973) to fit their data. Here, however, we allow diffusion limitations in the very thin catalytic layer. The temperature is assumed constant within the layer since the primary heat transfer resistance occurs in the fluid. The effectiveness factor curve is generated using a one-term collocation for small Thiele modules and the asymptotic solution for large Thiele modules (Finlayson, 1974).

The diffusion in the catalytic layer is governed by

Larry C. Young is with Amoco Production Company, Tulsa, Oklahoma 74102.

Parts I and II of this paper appeared in *AIChE J.*, **22**, 331 (1976).

0001-1541-79-9439-0192-\$00.75. © The American Institute of Chemical Engineers, 1979.

$$\begin{aligned} D_s \frac{d^2c}{dx^2} &= \text{rate}[c(x)] \\ c &= y_o c_o \quad \text{at } x = \xi \\ \frac{dc}{dx} &= 0 \quad \text{at } x = 0 \end{aligned} \quad (2)$$

By introducing  $c = y c_o$ , with  $y$  the mole fraction carbon dioxide, and setting  $y_{O_2} = (E + y)2/3$  (with  $E = 0.03$ , assuming  $y_{CO}/y_{H_2}$  remains constant), we can nondimensionalize this equation to give

$$\begin{aligned} \frac{d^2y}{ds^2} &= \phi^2 f(y) \\ y &= y_o \quad \text{at } s = 1 \end{aligned} \quad (3)$$

$$\frac{dy}{ds} = 0 \quad \text{at } s = 0$$

$$\phi^2 = \frac{\xi^2 k_o g(y_o)}{D_s C_o}, \quad f(y) = \frac{g(y)}{g(y_o)} \quad (4)$$

with

$$g(y) = \frac{(E + y)y}{(1 + \alpha y)^2} \quad (5)$$

The asymptotic solution is

$$\begin{aligned} \eta &= \frac{\sqrt{2}}{\phi} \left[ \int_0^{y_o} f(y) dy \right]^{1/2} \\ &= \frac{\sqrt{2}}{\phi} \frac{1}{g(y_o)} \left\{ \frac{E}{\alpha^2} \left[ \frac{1}{1 + \alpha y} + \log_e(1 + \alpha y) \right] \right. \\ &\quad \left. + \frac{1}{\alpha^3} \left[ 1 + \alpha y - 2 \log_e(1 + \alpha y) - \frac{1}{1 + \alpha y} \right] \right\}^{1/2} \Big|_0^{y_o} \quad (6) \end{aligned}$$

The reader desiring other details of the model is referred to Young & Finlayson (1967a, b).

### PARAMETRIC STUDY

The hysteresis effect is illustrated in Figure 1. Such curves have been obtained experimentally by Hlaváček and Votruba (1974) and Mosterky et al. (1974) in the following manner. Beginning with a cold reactor, desired inlet conditions are maintained at a low temperature until steady state has been reached, giving one data point on

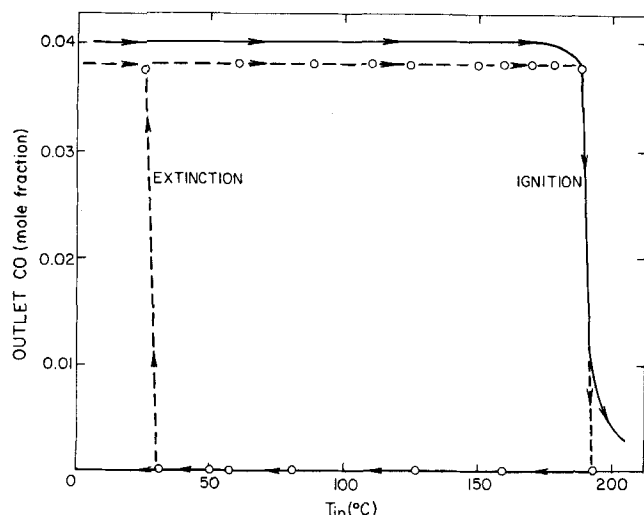


Fig. 1. Hysteresis curve, ○ experimental data, — theory.  $Re = 152$ ,  $L = 0.06$  m,  $\epsilon = 0.23$ ,  $\xi = 0.0279$  mm,  $r_h = 0.749$  mm,  $D = 1.63 \times 10^{19}/T$ ,  $k_f/k_s = 0.225$ ,  $y_{Co,in} = 0.04$ .

TABLE 1. IGNITION AND EXTINCTION TEMPERATURES FOR DIFFERENT GEOMETRIES, P1 KINETICS

| Geometry  | $T_{ex}(^{\circ}C)$ | $T_{ig}(^{\circ}C)$ | $\Delta T(^{\circ}C)$ |
|-----------|---------------------|---------------------|-----------------------|
| Square    | 302                 | 308                 | 6                     |
| Circle    | 309                 | 309                 | 0                     |
| Trapezoid | 309                 | 312                 | 3                     |
| Rectangle | 314                 | 314                 | 0                     |

the top part of the curve. Then the inlet temperature is raised, and the experiment again proceeds to steady state, giving another data point. This procedure is followed giving the curve denoted by  $\rightarrow$ . At the ignition temperature, light off occurs, and the concentration of carbon monoxide out of the reactor decreases drastically. Almost complete conversion is obtained for any higher inlet temperature. Then the inlet temperature is lowered, step by step, giving rise to the curve marked  $\leftarrow$ . At the extinction temperature the concentration suddenly increases and little reaction takes place. The profiles shown in Figure 1 then represent two cases, one with light off and the other nearly extinguished.

The hysteresis is expressed in terms of extinction and ignition temperatures. The ignition temperature is the minimum inlet fluid temperature needed to cause the reaction to light off if the reactor starts cold. The extinction temperature is the temperature below which the reaction rate essentially ceases, even if the reactor starts hot. We determine these two extremes by solving the steady state problem. The solution depends on the initial guess. We use an initial guess for concentration and temperature as the inlet values (no reaction) to determine the ignition temperature and the adiabatic temperature and no reactant to find the extinction temperature. We emphasize that the source of hysteresis in these models is the axial conduction of heat in the wall. The base case, unless otherwise noted, is  $Re = 160$ ,  $y_{Co,inlet} = 0.04$ , P2 kinetics, square geometry,  $k_f/k_s = 0.04$ ,  $D_f/D_s = 20$ .

The first situation we investigate is the reaction rate expression. In Young and Finlayson (1976b) most calculations used a less realistic reaction rate expression

$$\text{rate for P1} = \frac{A y_{O_2} y_{CO}}{y_{O_2} + \alpha y_{CO}^2 \exp(B/T)} \quad (7)$$

Shown in Figure 2 is the hysteresis curve for P1 and P2

kinetics. Clearly, the more realistic P2 kinetics shows more hysteresis.

The effect of geometry is illustrated for P1 kinetics only in Table 1. The effect of the shape of the duct is not great, although its importance could be bigger for P2 kinetics. Henceforth, we use P2 kinetics for square ducts.

Since the mechanism for hysteresis is due to axial conduction of heat in the wall, the hysteresis should decrease as  $k_s$  or the wall thickness decrease. The parameter which determines the magnitude of axial conduction effects is

$$\frac{k_s}{k_f} \cdot \frac{2r_h^2}{L^2} \frac{1-\epsilon}{\epsilon} \quad (8)$$

and so changes of  $\epsilon$  (changing the wall thickness) or  $k_s$  have similar effects. Shown in Table 2 is the effect of  $k_s$ , and here it needs to be about one-hundred times as small as the fluid  $k_f$  for the axial conduction effect to disappear. This result is particularly important in view of the general impression left by Young and Finlayson (1976b). There, most calculations were P1 kinetics, for which axial conduction is not an important phenomena (see Figure 2). With the more realistic P2 kinetics, Equation (1), however, axial conduction is very important and leads to the very wide hysteresis shown in Figure 1. The hysteresis is  $112^{\circ}C$  for 4% carbon monoxide.

The effect of flow rate is illustrated in Figure 3. As flow rate increases, the ignition temperature increases

TABLE 2. IGNITION AND EXTINCTION TEMPERATURES FOR DIFFERENT WALL THERMAL CONDUCTIVITIES

| $k_f/k_s$ | $T_{ex}(^{\circ}C)$ | $T_{ig}(^{\circ}C)$ | $\Delta T(^{\circ}C)$ |
|-----------|---------------------|---------------------|-----------------------|
| 0.01      | 218                 | 326                 | 108                   |
| 0.04      | 214                 | 326                 | 112                   |
| 1.0       | 293                 | 326                 | 33                    |
| 100       | 324                 | 324                 | 0                     |

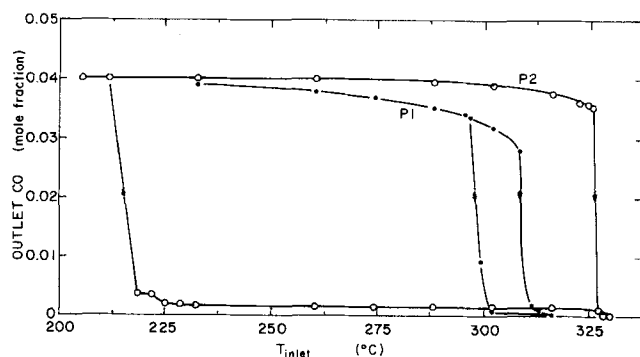


Fig. 2. Effect of reaction rate expression.

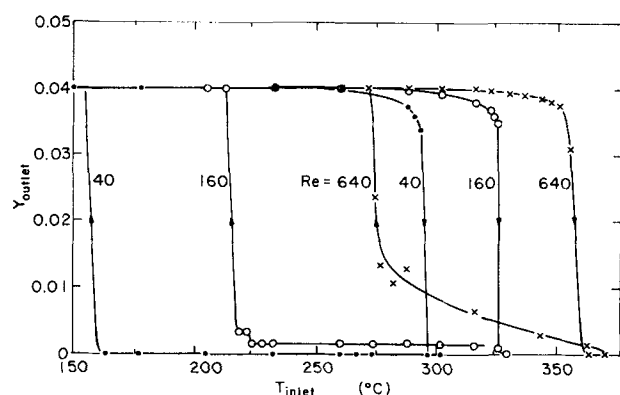


Fig. 3. Effect of flow rate.

TABLE 3. IGNITION AND EXTINCTION TEMPERATURES FOR DIFFERENT INLET MOLE FRACTIONS

| Mole fraction<br>CO inlet | $T_{ex} (^{\circ}\text{C})$ | $T_{ig} (^{\circ}\text{C})$ | $\Delta T (^{\circ}\text{C})$ |
|---------------------------|-----------------------------|-----------------------------|-------------------------------|
| 0.01                      | 319                         | 319                         | 0                             |
| 0.02                      | 312                         | 326                         | 14                            |
| 0.04                      | 214                         | 326                         | 112                           |

TABLE 4. IGNITION AND EXTINCTION TEMPERATURES FOR DIFFERENT EFFECTIVE DIFFUSIVITIES IN CATALYTIC LAYER

| $D_f/D_s$ | $T_{ex} (^{\circ}\text{C})$ | $T_{ig} (^{\circ}\text{C})$ | $\Delta T (^{\circ}\text{C})$ |
|-----------|-----------------------------|-----------------------------|-------------------------------|
| 20        | 214                         | 326                         | 112                           |
| 70        | 279                         | 326                         | 47                            |

slightly, and the extinction temperature increases more drastically. The net effect is to narrow the temperature range over which hysteresis is possible. The extinction curve for  $Re = 640$  shows that emission breakthrough has occurred, even though the reactor has lit off, the exiting fluid still contains appreciable unreacted carbon monoxide due to mass transfer limitations.

The effect of carbon monoxide concentration is shown in Table 3. Hysteresis is enhanced by high levels of carbon monoxide. This agrees with the experimental results.

Finally, the effect of diffusivity in the porous catalytic layer is demonstrated in Table 4. A lower effective diffusivity in the solid reduces the reaction rate at high temperature, which decreases the range of hysteresis.

#### COMPARISON TO EXPERIMENTAL DATA

The experimental data of Hlaváček and Votruba (1974) is shown in Figure 1. When the inlet concentration is 4% carbon monoxide, the reactor can light off at room temperature; that is, if the reactor starts out hot, an inlet temperature of room temperature causes ignition. If the reactor is initially cold, an extinguished state is also possible at room temperature. The data show a small conversion for the extinguished state, which may be an artifact or due to reaction outside the reactor itself. Calculations were done using model II-A (transverse conduction in fluid, axial conduction in solid) and model II (transverse conduction in fluid). The reaction rate expression, Equation (1), was used, along with an assumed value of  $D_s$ . We have no evidence that this is appropriate for the platinum catalyst used experimentally, since no reaction rate data were given by Hlaváček and Votruba (1974). We used the dimensions of the experimental reactor and the experimental flow rate and inlet conditions. We assumed a thermal conductivity for the wall, which was stated as porous alumina (holes were drilled directly into it). The activity of the catalyst and the depth of platinum ( $\zeta$ ) were unknown. We assumed a reasonable value for  $\zeta$  based on previous work by Young and Finlayson, (1976b). The activity of the catalyst was determined by fitting the calculated curve to the data for  $y_{CO, in} = 0.04$ ,  $T_{in} = 190^{\circ}\text{C}$ . Thus, the right-hand side of the 4% curve in Figure 1 is fit by parameter choice. [Here, the catalyst is 350 times more active than that used by Young and Finlayson (1976b)]. The rest of the calculated curves are thereby determined; there are no more adjustable parameters.

The calculations for 4% carbon monoxide indicate that light off can occur at room temperature, as in the data. The experimental results are not clear as to the extinction

temperature. Calculations were not done for inlet temperatures below room temperature ( $25^{\circ}\text{C}$ ), but the calculations indicate the extinction temperature is below room temperature. Thus, the data and calculations agree that the reactor can be ignited from room temperature ( $25^{\circ}\text{C}$ ) to  $190^{\circ}\text{C}$ .

The calculations and data for 2% carbon monoxide are compared in Figure 4 and indicate that ignition occurs at  $187^{\circ}\text{C}$  (vs.  $182^{\circ}\text{C}$  experimentally) and that extinction occurs at  $136^{\circ}\text{C}$  (vs.  $118^{\circ}\text{C}$  experimentally). The fact that the region of hysteresis narrows at lower carbon monoxide concentration is correctly modeled.

In view of the uncertainty of some of the parameter values, we regard the agreement with the data as quite adequate. The model is qualitatively correct and is capable of fitting the data. Based on the results given below, we can say that the essential features of the model are the inclusion of transverse conduction in the fluid, axial conduction in the wall, and the use of the kinetics expression, Equation (1). The regions of hysteresis are affected by  $k_s$ , the solid thermal conductivity,  $\epsilon$ , the void fraction, and  $D_s$ , the effective diffusivity in the solid.

#### MODEL DISCRIMINATION

Young and Finlayson (1976b) presented several models and argued that the model which included transverse conduction and diffusion in the fluid and axial conduction in the wall was the correct one (model II-A). The models were called model I for a model with assigned Nusselt and Sherwood numbers, which are usually obtained as the asymptotic solutions to a Graetz type of problem with no chemical reaction. Model II included transverse conduction in the fluid (and transverse diffusion), with the argument being that in a Graetz problem if the wall temperature suddenly increases (as it does in the reactor at light off), the Nusselt number goes to infinity, and when that happens the multiple steady states predicted by model I are not possible. Using finite Nusselt and Sherwood numbers in this region, as is done in model I, is incorrect. We can also add axial conductivity to both models to obtain models I-A and II-A. Despite the fact that the theoretical underpinnings of model I are weak, this model has been attractive to some because of its simplicity. We wish to examine further the question of which model is appropriate.

In model I we must solve the following equations:

$$\frac{dy^m}{dz} = 2\alpha_2 Sh (y^s - y^m) \quad (9)$$

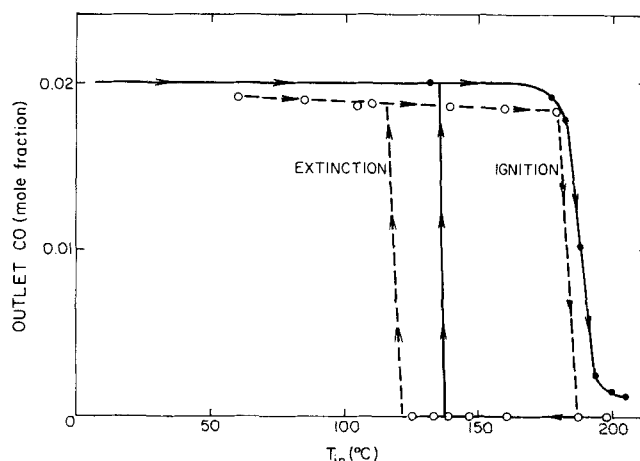


Fig. 4. Hysteresis curve, 2% carbon monoxide, other conditions as in Figure 1.  $\circ$  Experimental data, — theory.

$$\frac{dT^m}{dz} = 2\alpha_1 Nu (T^s - T^m) \quad (10)$$

$$Sh (y^m - y^s) = -2\alpha_6 \beta_4 \langle r \rangle \quad (11)$$

$$Nu (T^m - T^s) = 2\beta_5 \langle r \rangle \quad (12)$$

The solution to Equations (11) and (12) need not be unique. For the parameter values used here, model I predicts multiple steady states which are qualitatively similar to those illustrated in Figures 1 and 4. Unfortunately, model I predicts an infinite number of stable steady states between the highest and lowest ones (Liu and Amundson, 1962). In agreement with Eigenburger (1972), we find that the addition of axial conduction to model I (giving model I-A) reduces the maximum number of steady states to at most two, one similar to the highest steady state of model I and possibly one similar to the lowest steady state of model I. The lower steady state of model I-A occurs only when the lowest steady state of model I does not exhibit light off. Thus, for steady calculations, models I and I-A are similar provided the correct steady state(s) of model I is chosen.

The addition of transverse conduction and diffusion to model I (giving model II) results in a model which predicts that multiple steady states do not occur. The single steady state of model II is always similar to the lowest steady state of model I. Thus, for steady state calculations, models I and II are similar provided the lowest steady state of model I is chosen. This choice is different from the one model I-A indicates we should elect.

Thus, the addition of axial conduction (model I-A) or transverse conduction and diffusion (model II) indicate that model I can be appropriate for steady state calculations; however, these two more complex models suggest that different steady states of model I should be selected. For a case when the lowest steady state of model I exhibits light off, model II suggests that this is the only steady state which is correct, while model I-A suggests that only the highest steady state of model I should exist.

Model II is obviously inappropriate for the experimental reactor performance illustrated in Figures 1 and 4, since it can only predict a single steady state. Model I-A can predict hysteresis of the type illustrated in Figures 1 and 4. Even though model I obviously contains incorrect physical assumptions, it can also predict hysteresis of the type illustrated in Figures 1 and 4. Since models I and I-A are sometimes favored over model II-A owing to their simplicity, it is important to determine whether they can predict the correct influence of the model parameters on the magnitude of the hysteresis. Since models I and I-A predict approximately the correct ignition temperature, we will concentrate on the question of whether they predict the correct extinction temperature.

From Table 5 it is apparent that model I predicts approximately the correct influence of inlet carbon monoxide concentration on extinction temperature. Model I will not, however, predict the correct influence of flow rate on extinction temperature. To illustrate this problem, we combine Equations (9) to (12) for the case of  $\alpha_1 = \alpha_2$  (appropriate for gases, with  $Pr = Sc$ ):

$$y^s = y_o + (T_o - T^s) \alpha_6 \beta_4 / \beta_5 \quad (13)$$

$$T^m = T^s + 2\beta_5 \langle r(y^s, T^s) \rangle / Nu \quad (14)$$

Note that in Equations (13) and (14) the flow rate does not appear. Equations (13) and (14) can be used to determine whether an upper and lower steady state exists for model I at the inlet conditions. The minimum

TABLE 5. HYSTERESIS FOR DIFFERENT MODELS OF EXPERIMENTAL CONDITIONS. TEMPERATURES IN °C

| $y_{CO,o}$     | Exp | II-A | II  | I-A | I   |
|----------------|-----|------|-----|-----|-----|
| 0.04 ignition  | 190 | 186  | 189 | 185 | 192 |
| 0.02           | 182 | 186  | 187 | 179 | 188 |
| 0.01           | 175 | 174  | 174 | 174 | 182 |
| 0.4 extinction | ~21 | <21  | 189 | <21 | <21 |
| 0.02           | 118 | 137  | 187 | 100 | 108 |
| 0.01           | 129 | 174  | 174 | 169 | 168 |

inlet temperature at which an upper steady state exists will be only slightly greater than the extinction temperature, since a change in inlet temperature of approximately 20°C is sufficient to move the reaction zone from the front of the converter to the back (see Figure 5). In contrast to the prediction of model I, Figure 3 shows that model II-A predicts a substantially greater influence of flow rate on extinction temperature. The effects predicted by model II-A tend to be supported by the experimental data in Figure 6 (Mosterky et al., 1974). The physical explanation for this discrepancy is that in model I the velocity acts only as a scale for the converter length (through  $\alpha_1$  and  $\alpha_2$ ), whereas in model II-A velocity not

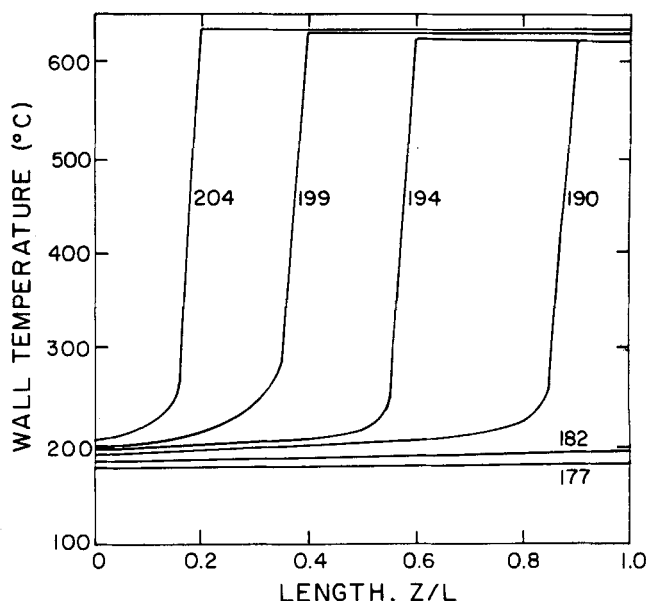


Fig. 5. Temperature profile in reactor. Model II (no axial conduction). Values shown are  $T_{in}$  (°C), parameters for experimental reactor.

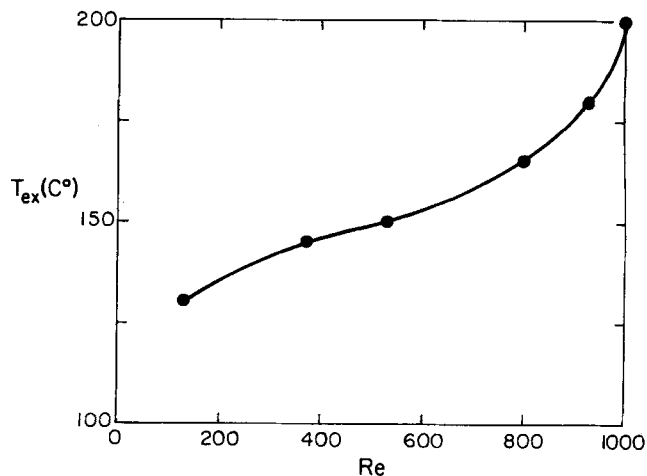


Fig. 6. Extinction temperature for experimental data (5).  $y_{CO,inlet} = 0.01$ .

only scales the converter length but also reduces the effect of axial conduction. The source of hysteresis in this reactor is axial conduction. Model I predicts multiple steady states due to a combination of physically incorrect assumptions. The fact that model I predicts approximately the correct hysteresis in Table 5 is fortuitous. For different parameters (wall thickness, kinetic expression, flow rate, etc.) this agreement would not occur.

Model I-A contains axial conduction, so one might think that it can predict the correct influence of the parameters on extinction. This assumption would be incorrect. Transverse conduction and diffusion tend to increase the extinction temperature, while axial conduction decreases it. Thus, the extinction temperature for model II-A is always between those for models I-A and II. If the parameters are changed so that axial conduction becomes less important (for example, increased velocity, decreased wall thickness, etc.), the extinction temperature for model II-A will move continuously toward that for model II. On the other hand, the extinction temperature for model I-A will never be less than that for model I, because the upper steady state of model I-A is near the highest steady state of model I (see Eigenberger, 1972). Model I-A predicts the correct extinction temperatures only when axial conduction effects are very large, whereas for model parameters of interest, both axial conduction and transverse conduction and diffusion are important.

## CONCLUSION

The parametric sensitivity of model II-A has been determined. Hysteresis is enhanced by high carbon monoxide levels and low flow rates. The model agrees qualitatively with experimental data. The reaction rate expression (1) and axial conduction in the walls have a crucial effect on comparison with experimental data. The simplest model I is not appropriate to cases with multiple steady states, since it predicts an extinction temperature essentially independent of flow rate, in contradiction to experimental data.

## ACKNOWLEDGMENT

Acknowledgment is made to the donors of the Petroleum Research Fund, administered by the American Chemical Society, for support of this research under grant PRF No. 7698-AC7.

## NOTATION

|             |   |
|-------------|---|
| $A$         | = constant in reaction rate expression, K   |
| $B$         | = constant in reaction rate expression, K   |
| $C$         | = concentration, kg · mole/m <sup>3</sup>   |
| $C_o$       | = inlet concentration of gas, kg · mole/m <sup>3</sup>  |
| $D$         | = rate constant, kg · mole/sm <sup>3</sup> K, $4.67 \times 10^{16}/T$ ( $1.63 \times 10^{10}/T$ ) |
| $D_f$       | = diffusivity of carbon monoxide in air, m <sup>2</sup> /s  |
| $D_s$       | = effective diffusivity of carbon monoxide in catalytic layer, m <sup>2</sup> /s                  |
| $E$         | = inlet oxygen concentration is $E + y_{CO, in}$  |
| $f(y)$      | = function defined in Equation (4)  |
| $G$         | = mass flux, kg/m <sup>2</sup> s  |
| $g(y)$      | = function defined in Equation (5)  |
| $-\Delta H$ | = heat of reaction, $3.37 \times 10^8$ J/(kg mole CO + 1/3 kg mole H <sub>2</sub> )               |
| $h^*$       | = heat transfer coefficient, J/sm <sup>2</sup> K  |
| $k_o$       | = rate constant = $D \exp(-A/T)$  |
| $k_f$       | = fluid thermal conductivity, J/smK   |
| $k_s$       | = solid thermal conductivity (J/smK), $k_s = k_f/$  |

$$0.04 (k_s = k_f/0.225)$$

|                     |   |
|---------------------|---|
| $k^*$               | = mass transfer coefficient, m/s                                  |
| $L$                 | = length of monolith, 0.102 m (0.06 m)                            |
| $Nu$                | = Nusselt number, $4r_h h^*/k_f$                                  |
| $Pe_h$              | = Peclet number for heat, $Pr Re$                                 |
| $Pe_m$              | = Peclet number for mass, $Sc Re$                                 |
| $\langle r \rangle$ | = reaction rate, kg · mole/sm <sup>3</sup>                        |
| $r_h$               | = hydraulic radius, duct open area/perimeter, 0.305 mm (0.749 mm) |
| $Re$                | = Reynolds number, $4r_h G/\mu$ , 160 (152)                       |
| $s$                 | = dimensionless distance in catalytic layer, $x/\xi$              |
| $Sh$                | = Sherwood number, $4r_h k^*/D_f$                                 |
| $T$                 | = temperature, K  |
| $x$                 | = distance in catalytic layer, m                                  |
| $y_i$               | = mole fraction of species $i$                                    |
| $y_o$               | = inlet mole fraction of carbon monoxide                          |

## Greek Letters

|            |  |
|------------|--|
| $\alpha$   | = constant in reaction rate expression, $\alpha = C' \exp(B/T)$  |
| $\alpha_1$ | = dimensionless thermal converter length, $L/(2r_h Pe_h)$ , 1.49 (0.376)                                     |
| $\alpha_2$ | = dimensionless mass converter length, $L/(2r_h Pe_m)$ , 1.49 (0.376)  |
| $\alpha_6$ | = $(D_s/D_f)(2r_h/\xi)$ , 2 (2.68)   |
| $\beta_4$  | = $\xi^2/CD_s$ , $2.02 \times 10^{-10}$ m <sup>3</sup> s/kg ( $6.79 \times 10^{-10}$ )                       |
| $\beta_5$  | = $-\Delta H_{rxn} 2r_h \xi/k_f$ , $4.35 \times 10^{-6}$ m <sup>3</sup> sK/kg mole ( $1.97 \times 10^{-5}$ ) |
| $\epsilon$ | = void fraction of reactor, 2/3 (0.23)   |
| $\xi$      | = thickness of catalytic layer, 0.0152 mm (0.0279 mm)  |
| $\eta$     | = effectiveness factor, rate at bulk conditions/(average rate in catalytic layer)                            |
| $\mu$      | = gas viscosity, kg/ms   |
| $\phi$     | = Thiele modulus, $\xi^2 k_o g(y_o)/(D_s C_o)$   |

## Superscripts and subscripts

|     |                       |
|-----|-----------------------|
| $s$ | = solid value         |
| $m$ | = average fluid value |
| $o$ | = inlet value         |

## LITERATURE CITED

- Eigenberger, G., "On the Dynamic Behavior of the Catalytic Fixed-Bed Reactor in the Region of Multiple Steady States—I. The Influence of Heat Conduction in Two Phase Models," *Chem. Eng. Sci.*, **27**, 1909 (1972).
- Finlayson, B. A., "Orthogonal Collocation in Chemical Reaction Engineering," *Cat. Rev.—Sci. Eng.*, **10**, 69 (1974).
- Hlaváček, V., and J. Votruba, "Experimental Study of Multiple Steady States in Adiabatic Catalytic Systems," in *Chemical Reaction Engineering—II*, H. M. Hulburt, ed., pp. 545-558, Am. Chem. Soc. Ser. 133 (1974).
- Liu, S. L., and N. R. Amundson, "Stability of Adiabatic Packed Bed Reactors. An Elementary Treatment," *Ind. Eng. Chem. Fundamentals*, **1**, 200 (1962).
- Mosterky, J., V. Hlaváček, and J. Votruba, "Experimentallstudie der Kohlenmonoxidoxidation an einem Waffenrohrkatalysator," *Erdöl und Kohle*, **27**, 261 (1974).
- Voltz, S. E., C. R. Morgan, D. Liederman, and S. M. Jacob, "Kinetic Study of Carbon Monoxide and Propylene Oxidation on Platinum Catalysts," *Ind. Eng. Chem. Prod. Res. Develop.*, **12**, 294 (1973).
- Young, L. C., and B. A. Finlayson, "Mathematical Models of the Monolith Catalytic Converter: Part I. Development of Model and Application of Orthogonal Collocation," *AIChE J.*, **22**, 331 (1976a).
- , "Mathematical Models of the Monolith Catalytic Converter: Part II. Application to Automobile Exhaust," *ibid.*, **22**, 343 (1976b).

\* The numbers listed are for the base case. The numbers in parentheses are the values used for modelling the experimental data.

Manuscript received July 13, 1977; revision received February 6, and accepted June 8, 1978.